SPIE Liquid Crystals II
ANL/CHM/CP-96855

Charge transfer reactions in nematic liquid crystals

CONF-980731--

Gary P. Wiederrecht[a], Michael R. Wasielewski[a,b], Tamar Galili[c], and Haim Levanon[c]

[a]Chemistry Division, Argonne National Laboratory, Argonne, IL 60439-4831
[b]Department of Chemistry, Northwestern University, Evanston, IL 60208-3113
[c]Department of Physical Chemistry, The Hebrew University of Jerusalem, Jerusalem, Israel 91904

ABSTRACT

Ultrafast transient absorption studies of intramolecular photoinduced charge separation and thermal charge recombination were carried out on a molecule consisting of a 4-(*N*-pyrrolidino)naphthalene-1,8-imide donor (PNI) covalently attached to a pyromellitimide acceptor (PI) dissolved in the liquid crystal 4'-(n-pentyl)-4-cyanobiphenyl (5CB). The temperature dependencies of the charge separation and recombination rates were obtained at temperatures above the nematic-isotropic phase transition of 5CB, where ordered microdomains exist and scattering of visible light by these domains is absent. We show that excited state charge separation is non-adiabatic, and obtain the unexpected result that charge separation is dominated by molecular reorientation of 5CB perpendicular to the director within the liquid crystal microdomains. We also show that charge recombination is adiabatic and is controlled by the comparatively slow collective reorientation of the liquid crystal microdomains relative to the orientation of PNI^{+}-PI^{-}. We also report the results of time resolved electron paramagnetic resonance (TREPR) studies of photoinduced charge separation in a series of supramolecular compounds dissoved in oriented liquid crystal solvents. These studies permit the determination of the radical pair energy levels as the solvent reorganization energy increases from the low temperature crystalline phase, through the soft glass phase, to the nematic phase of the liquid crystal.

Keywords: Liquid Crystals, Charge Transfer, Solvation Dynamics

1. INTRODUCTION

Molecular ordering has profound effects on the physical and chemical behavior of materials. Ordered materials can show highly applicable phenomena, such as uni-directional photoconductivity[1,2], bulk electrooptic character[3-5], and selectivity in solid-state chemical reactions[6], to name only a few. For many of these characteristics, charge transfer interactions within the medium are of critical importance. For example, significant molecular hyperpolarizabilities (β) are necessary to see a large second order nonlinearity in bulk ordered materials, and are typically found in molecules that have a high degree of electron donor-acceptor character.[7] Uni-directional photoconductivity for solar energy applications in organized organic media rely in large part on improvements in the efficiency of photoinduced charge separation and charge transport.[8] These considerations also extend to natural systems, such as photosynthetic reaction centers, where anisotropic environments are employed to promote efficient, photoinduced charge separation over large distances.[9] Therefore, efforts to more fully understand the effect of anisotropic environments on charge transfer reactions are particularly relevant for understanding and improving materials' performance in a variety of scientifically interesting and applicable fronts.[10-12]

A disadvantage of charge separation reactions in solid materials is that the solid "solvent" that mediates these reactions cannot reorient to stabilize an ion pair. This has been shown to destabilize the energy of ion pairs in solid-state environments relative to liquids by approximately 0.8eV.[13] As a result, many solid state charge separation reactions are rendered unfeasable or inefficient by allowing other pathways to occur, such as radiative or non-radiative decay of an excited state. Therefore, significant efficiency improvements in technologically applicable materials could be achieved if materials can be found which utilize the advantages of solvent dipole reorientation to stabilize ion pairs in liquids, while maintaining an anisotropic environment. Liquid crystals provide a unique opportunity in this regard. They are generally good solvents, chemically stable, and frequently commercially available. They are also easily aligned in the presence of a silane surfactant

DISCLAIMER

on glass or a magnetic field, thus avoiding more complex procedures such as crystal growing. As a result, they are already utilized as a spectroscopic tool to study the behavior of aligned, nonlinear optical molecules that are doped into the liquid crystals. [14] Furthermore, cooperative interactions between the liquid crystal molecules themselves show a wide range of nonlinear behavior that charge separation reactions can serve to enhance.[4,15-20] However, there are surprisingly few studies in the literature that explore the mechanisms of charge transfer reactions in liquid crystal solvents.[10-12,21]

Two projects are introduced here which illustrate the novel behavior of intramolecular electron transfer reactions in liquid crystal solvents. In the first series of experiments, ultrafast transient absorption studies of intramolecular photoinduced charge separation and thermal charge recombination were performed for molecules dissolved in the isotropic phase of a liquid crystal solvent, just above the nematic to isotropic phase transition.[12] In this region, ordered microdomains give rise to solvation dynamics that consist of collective reorientational motions of the microdomains and relatively faster reorientations of molecules within the domains. We show that the different temperature dependence of these responses permits the assignment of particular types of solvent motions as mediators of charge transfer and charge return events.

In the liquid crystal and solid phases of these solvents, intramolecular electron transfer rates are reduced by several orders of magnitude (from ps to ns), permitting the observation of intramolecular electron transfer processes on sub-microsecond time scales through time-resolved electron paramagnetic resonance (TREPR) spectroscopy. In the second series of experiments, we show that temperature dependent intramolecular electron transfer studies of biomimetic molecules in liquid crystals permit gradual tuning of the solvent reorganization energy (λ_s) by 0.6 eV. Thus, the branching ratio of the electron transfer rates between singlet- or triplet-initiated routes can be controlled, and the absolute values of the energy levels of radical pair states in supramolecular systems can be determined.

2. EXPERIMENTAL METHODS

For the first series of experiments, ultrafast transient absorption studies of intramolecular photoinduced charge separation and thermal charge recombination were carried out on a molecule consisting of a 4-(*N*-pyrrolidino)naphthalene-1,8-imide donor (PNI) covalently attached to a pyromellitimide acceptor (PI) dissolved in the liquid crystal 4'-(n-pentyl)-4-cyanobiphenyl (5CB), as shown in Figure 1. Time-resolved transient absorption studies were performed with a Ti:sapphire laser system that excited PNI with 400 nm, 120 fs pulses.[22] The temperature dependencies of the charge separation and recombination rates were obtained at temperatures above the nematic-isotropic phase transition of 5CB, where ordered microdomains exist and scattering of visible light by these domains is absent. The PI acceptor has a distinctive absorption band at 710 nm when reduced, permitting unambiguous assignment of the final radical ion pair state.[23,24]

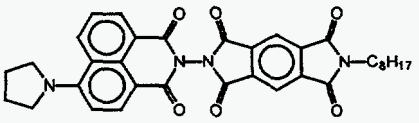

PNI-PI

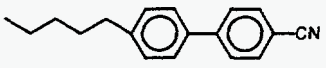

5CB

Figure 1. The charge transfer molecule PNI-PI and the liquid crystal solvent molecule 5CB are illustrated.

The second series of experiments deals with a series of covalently linked compounds (Figure 2) containing a chlorophyll-like (chlorin) electron donor, D (ZC). Two electron acceptors are used with different reduction potentials, i.e., pyromellitimide, A_1 (PI) and 1,8:4,5 naphthalenediimide, A_2 (NI) to produce a series of molecules with small but deliberate differences of the ion-pair energies. The compounds investigated are ZCPI, ZCNI and ZCPINI, with D-to-A_1, D-to-A_2 and D-to-A_2 center-to-center distances of ~ 11, ~ 11 and ~ 18 Å, respectively (for conciseness the spacer is not mentioned in the acronyms). These compounds, when oriented in different LCs, show photoinduced IET to produce charge-separated states that can be monitored by TREPR. The origin of such a state and the spin dynamics associated with it strongly depend not only on λ_s, but very substantially on the molecular architecture. Thus, while ZC^{+}- PI^{-} and ZC^{+}- NI^{-}, with short donor-acceptor distances, exhibit triplet radical pair (TRP) spectra, i.e., $^3[D^{+}- A^{-}]$, the much longer donor-acceptor distance in the triad, ZC^{+}-PI-NI^{-}, results in a correlated radical pair (CRP) spectrum, i.e., $^{1,3}[D^{+}- A_1- A_2^{-}]$. These two types of spectra can be differentiated only by TREPR, via the dipolar and/or the exchange interactions, which strongly depend on the donor-acceptor distance. We further show that the spectral analysis in terms of the energy states scheme in Figure 3, illustrating the different routes of triplet and RP states production, permits an accurate assignment of the energies of the RPs in the different phases of the LC solvents.

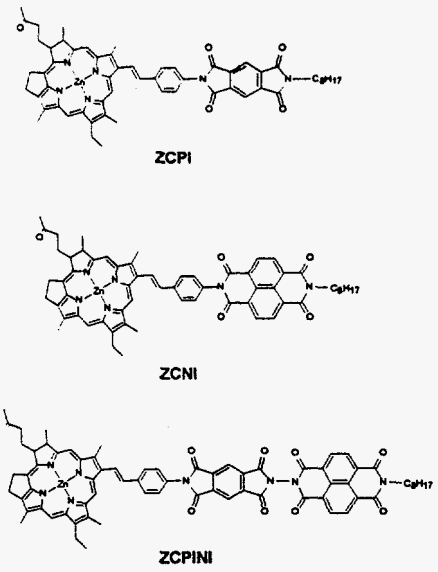

Figure 2. The supramolecular charge transfer systems are illustrated.

During these experiments two sample orientations were studied, **L** || **B** and **L** ⊥ **B**, where **L** is the director of the LC. The sign of the diamagnetic susceptibility determines the relationship between **L** and **B** in the nematic phase, i.e., $\Delta\chi = \Delta\chi_{\|}-\Delta\chi_{\perp}$. A positive $\Delta\chi$ causes the initial alignment to be **L** || **B**, which is the case for E-7. A negative $\Delta\chi$ leads to an **L** ⊥ **B** initial alignment, which is the case for ZLI-1167. A LC characterized by a negative $\Delta\chi$ is also referred to as a "multi-domain" configuration, due to the fanning of the directors of the LC in the plane perpendicular to **B**. Spectra for **L** ⊥ **B** in E-7 can also be obtained when the sample is held below the freezing temperature. This is obtained by rotation of the sample in the microwave cavity by $\pi/2$ about an axis perpendicular to the external magnetic field. However, in the fluid nematic phase, rotation of the sample from the **L** || **B** position does not effect the spectral line shape due to molecular reorientation back to the initial parallel orientation.

The phase diagram of a nematic LC (e.g., E-7) exhibits three distinct phases with well-defined transition temperatures. Qualitatively, we define an additional phase, referred to as the soft glass (SG), which is found at higher temperatures within the crystalline phase. This regime is characterized by limited molecular motion. This phenomenon has been previously observed in other TREPR experiments in frozen liquid crystals.[25] The other LC, ZLI-1167, does not exhibit the soft glass characteristics of E-7, but exhibits an additional smectic phase. The reason for employing this LC is to check and differentiate between the spin polarization mechanisms that are operative using the donor-acceptor systems studied here. The phase transition temperatures for both LCs are:

E-7:

	210 K		263 K		333 K	
crystalline	→	soft-glass	→	nematic	→	isotropic

ZLI-1167:

	287 K		305 K		356 K	
crystalline	→	smectic	→	nematic	→	isotropic

The redox potentials for ZCPI, ZCNI, and ZCPINI were determined in benzonitrile/0.1M tetra-n-butylammonium perchlorate at a Pt electrode referenced to a saturated calomel electrode (SCE) using cyclic voltammetry. The electrochemical data given in Table 1 illustrates the relative RP energies of the three compounds, i.e., ZC^{+}-PI^{-} > ZC^{+}-NI^{-} > ZC^{+}-PI-NI^{-}. In other words, ZCPINI has the largest free energy change (ΔG) for singlet-initiated charge separation. An explanation is warranted for the increased driving force for charge separation of ZC^{+}-PI-NI^{-} vs. ZC^{+}-NI^{-}. The reduction potential values for the electron acceptors in benzonitrile are given in Table 1. Note that the NI acceptor is more easily reduced by 0.19 eV when coupled to PI, leading to a considerably larger driving force for electron transfer and faster electron separation within the triad than within the dyads.[24] The increased coupling between the two acceptors in ZCPINI is a simple method to achieve greater free energy for charge separation (CS) and lower free energy for charge recombination (CR). Table 1 also reports the free energies for charge-separation and energy levels of the RPs for

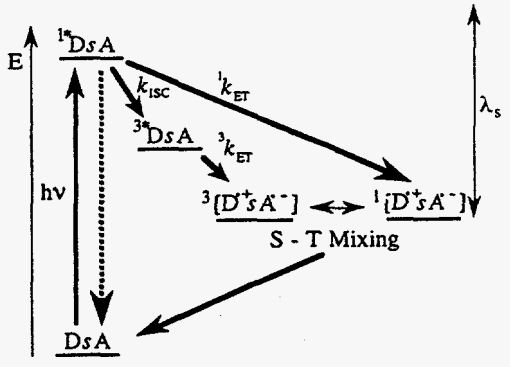

Figure 3. Energy level diagram of the IET reactions, valid for all donor-spacer- acceptor molecules. The solvent reorganization energy is represented schematically by λ_s.

the dyads and triad in the isotropic phase of E-7, as calculated from the following equations: [13,26]

$$\Delta G_{CS} = E_{OX} - E_{RED} - e0^2/\varepsilon_S r_{12} - E_S \quad (1)$$

$$\Delta G_{CR} = -\Delta G_{CS} - E_S = -E_{RP} \quad (2)$$

Here, E_S is the first excited singlet-state energy of the donor chromophore, E_{OX} is the oxidation potential of the electron donor, E_{RED} is the reduction potential of the electron acceptor, e_o is the electron charge, ε_s is the static dielectric constant, and r_{12} is the center-to-center distance between the donor and acceptor. The ΔG_{CS} and E_{RP} values for isotropic E-7 (Table 1) were calculated with ε_s = 19 (Merck Ltd.), E_s = 1.95 eV and E_{ox} = 0.43 eV.[24] Note that eq 1 is valid only in polar isotropic liquids where the solvent dipoles are free to reorient in the presence of a RP.[13] As a result, RP energies in low polarity solvents or crystalline environments are difficult to calculate accurately. The magnitude of this destabilization produces uncertainty about the absolute value of the RP energies. Recent work with a variety of porphyrin model systems indicate that the RPs are destabilized by approximately 0.8 eV in MTHF glass at low temperature relative to the isotropic solvent.[13]

We will show that the TREPR and electrochemical data permit the determination of the actual energy levels of the RPs with reasonable precision. This is determined by the energy level differences of the RPs under study. The assignment of these energy levels is based on the general scheme in Figure 2, namely: a) the singlet and triplet energy levels of the donor ZC (which is the same for all of the molecules under study); b) the appearance of the triplet (^{3}*ZC) and/or the triplet/singlet initiated RPs; and c) the electrochemical data given in Table 1.

Table 1. The reduction potentials of PI and NI in benzonitrile vs SCE; the free energies of charge-separation and RP energies calculated for isotropic E-7.

Molecule	Red. Pot. (eV)	r_{12} (Å)	ΔG_{CS} (eV)	E_{RP} (eV)
ZC^+- PI^-	-0.87	11	-0.72	1.23
ZC^+-NI^-	-0.60	11	-0.99	0.96
ZC^+-PI- NI^-	-0.41	18	-1.15	0.8

3. DISCUSSION

Charge transfer dynamics near nematic-isotropic phase transitions

Transient absorption kinetics of PNI-PI in 5CB and pyridine, two solvents with similar isotropic static dielectric constants, are shown in Figure 4. The figure clearly shows increased charge separation and recombination times in 5CB relative to those in pyridine. The inset to Figure 4 shows the transient absorption spectrum of PNI-PI in 5CB, which exhibits the characteristic PI^- absorption band at 710 nm indicative of the formation of PNI^+-PI^-. Figure 5 shows the results of a temperature dependence study of the charge separation and recombination times. The temperature was varied above the N-I phase transition from 310 K to 363 K. This figure shows that the charge recombination time constants strongly increase as the N-I phase transition is approached from higher temperatures, while the charge separation time constants increase only weakly.

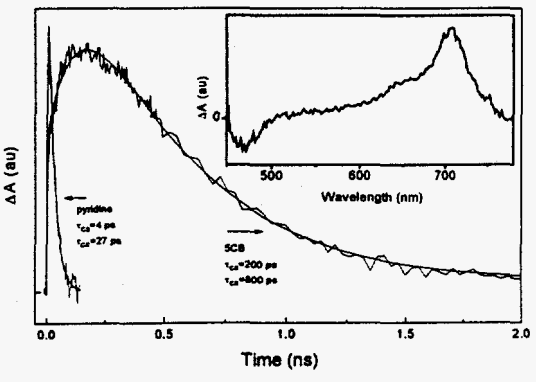

Figure 4. Transient absorption kinetics for PNI-PI in pyridine and in 5CB at 313K monitored at 710 nm. The inset shows the transient spectrum of PNI^+-PI^- in 5CB 150 ps after excitation.

In order to analyze this data, we use Landau-deGennes theory which shows that the molecular correlation length $\xi(T)$, is given by the relationship:[27]

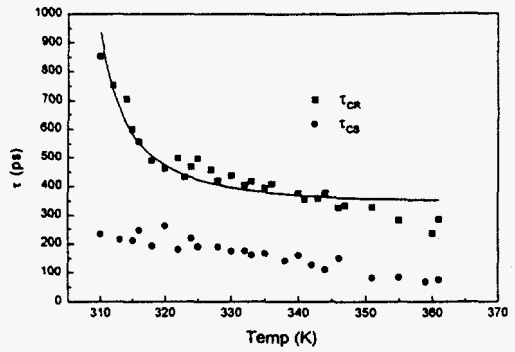

Figure 5. The temperature dependence of the time constants for charge separation (τ_{CS}) and charge recombination (τ_{CR}) for PNI-PI in 5CB are shown.

$$\xi(T) = \xi_o \left[\frac{T^*}{T - T^*} \right]^{1/2} \tag{3}$$

where ξ_o is a molecular length and T^* is just below the N-I phase transition. The N-I phase transition of 5CB containing 2×10^{-3}M PNI-PI was determined to be 306.5 K by differential scanning calorimetry (Perkin-Elmer Pyris 1). We use a value of 306 K for T^*. Equation 3 shows that molecular correlation lengths of approximately 20 exist just above the N-I phase transition and gradually decrease to 3 molecular lengths at 343 K. From eq. 3, the collective reorientation time τ_r of the microdomains has been shown to also change rapidly as the N-I phase transition is approached:[28]

$$\tau_r = \frac{\exp(E_a / k_B T)}{c(T - T^*)} \tag{4}$$

Here c is a constant and E_a is the activation energy for collective reorientation, which has been previously determined to be 34.3 kJ/mol for 5CB.[29] Equation 4 has been shown to be valid for 5CB up to 343 K, where small domain sizes begin to affect the dynamics of the liquid.[28] The data in Figure 5 was fit using eq. 2 plus an additive constant τ_{CR}^0 to account for the charge recombination time above the temperature where microdomains exist. E_a and T^* were fixed at 34.3 kJ/mol and 306 K, respectively, and only c and τ_{CR}^0 were varied. The fit to the data begins to err seriously only at temperatures above 343 K where Landau-deGennes theory is known to break down.[28] The identical temperature dependence of the charge recombination kinetics and the collective reorientational dynamics of the microdomains reveals that solvent controlled reaction dynamics are occurring and that charge recombination is adiabatic.

Although we have shown that the charge recombination times are controlled by the collective reorientation times of 5CB, the charge separation times are certainly not controlled by the same dynamics because no large increase of τ_{CS} is observed as the phase transition is approached. We can interpret the nature of the solvation mechanism for charge separation using the semi-classical Marcus equation for electron transfer:[30]

$$k_{CS} = \frac{2\pi V_{DA}^2 \exp(-\Delta G^* / k_B T)}{\hbar (4\pi\lambda k_B T)^{1/2}} \tag{5}$$

where $\Delta G^* = (\Delta G^0 + \lambda)^2 / 4\lambda$, V_{DA} is the electronic coupling matrix element between the donor and the acceptor, ΔG^* is the activation energy for electron transfer, ΔG^0 is the reaction free energy, and λ is the total reorganization energy, which is the sum of reorganization energies due to changes in solvation, λ_S and internal nuclear coordinates in the donor-acceptor pair, λ_i. Equation 3 assumes that the electron transfer reaction is non-adiabatic, which implies that the solvent motions that mediate charge transfer are fast compared to the rate of charge separation. If eq. 5 is obeyed, then a plot of $ln(k_{CS}T^{1/2})$ *vs.* $(1/T)$ should be a line with slope of $-\Delta G^*/k_B$. Using our data for the temperature dependence of the charge separation, such a plot is illustrated in Figure 6, and yields $\Delta G^* = 0.25$ eV. Since the plot in Fig. 6 is linear, it is clear that the charge separation reaction remains in the non-adiabatic regime, and thus, the retardation of the charge separation rate in 5CB relative to that of pyridine is a consequence of fast molecular motions that differ from the slower microdomain reorientational responses.

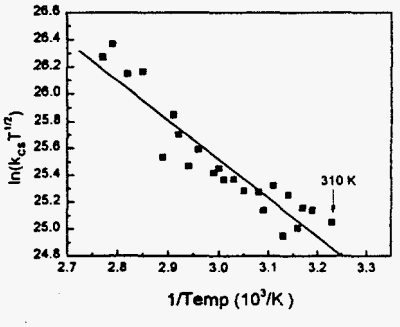

Figure 6. A plot of $ln(k_{CS}T^{1/2})$ *vs* $(1/T)$ for charge separation within PNI-PI in 5CB.

In order to slow the rate of charge separation, ΔG^0 and/or λ must differ significantly between 5CB and pyridine. Both ΔG^0 and λ depend on the dielectric properties of the medium. For 5CB the isotropic static dielectric

constant ε_S at temperatures slightly above the N-I transition is 10.5,[31] while that of pyridine is 12.5.[32] However, the rate of charge separation in 5CB is 50 times slower than that observed in pyridine. This suggests that the solvent microenvironment in 5CB at temperatures just above the N-I transition does not reflect the isotropic static dielectric constant for the medium.

For charge separation reactions it has been shown that ΔG^0 becomes more positive and λ_S decreases as ε_S decreases.[30,33] For charge separation reactions in continuous dielectrics ΔG^* can be related to ε_S by[13,34]

$$\Delta G^* = \left(\Delta G_E + \lambda_i + \frac{C}{\varepsilon_o}\right)^2 \Big/ 4C\left(\frac{1}{\varepsilon_o} - \frac{1}{\varepsilon_S}\right) \qquad (6)$$

where $C = e_o^2\left(\frac{1}{2r_D} + \frac{1}{2r_A} - \frac{1}{r_{DA}}\right)$ and $\Delta G_E = E_{ox}^D - E_{red}^A - E_S$. In these equations e_O is the electronic charge, ε_O is the high frequency dielectric constant of the medium, E_S is the lowest excited singlet state energy of PNI, E_{ox}^D and E_{red}^A are the one-electron oxidation and reduction potentials of PNI and PI, respectively, in polar media, r_D and r_A are the ionic radii of the donor and acceptor, respectively, and r_{DA} is the distance between them. For PNI-PI, E_S = 2.65 eV, E_{ox}^D = 1.09 V,[35] E_{red}^A = -0.80 V,[35] $r_D = r_A = 3.5 \pm 0.5$ Å,[36] and r_{DA} = 11 Å.[36] For both 5CB and pyridine $\varepsilon_O \cong 2.3$. Using λ_i = 0.3 eV[22] and the value of ΔG^* obtained from the data in Figure 6, eq. 6 can be solved to obtain an *effective* $\varepsilon_S = 6 \pm 3$ for the charge separation reaction in the 5CB microdomains. Since the anisotropic static dielectric constants for 5CB in its nematic phase are approximately $\varepsilon_\perp = 6$ and $\varepsilon_{//} = 18$,[31] our results suggest that motions of 5CB perpendicular to its director in the microdomains are sufficiently fast relative to charge separation within PNI-PI to promote rapid, non-adiabatic charge separation. Our results suggest that the anisotropic dielectric properties of liquid crystal solvents can be used to control the rates and mechanisms of electron transfer reactions. This is an important goal of research focused on the design of efficient photochemical charge separation and storage molecules.

TREPR in oriented liquid crystals

This series of experiments was performed as a function of temperature, beginning with the crystalline phase of the liquid crystals. The results of the temperature dependent study are summarized in Figure 7. The TREPR data in crystalline E-7 are consistent with driving forces for charge separation of the order given in Table 1, i.e., ZC^+-PI-NI^- > ZC^+-NI^- > ZC^+-PI^-. In further support for this argument, the EPR data indicate that the RP states of ZC^+-NI^- (exhibiting a weak EPR spectrum) and ZC^+-PI-NI^- are not formed via a triplet-initiated route. In other words, the energy levels lie below the ^{1}*ZCX state and above the ^{3}*ZCX energy level. Moreover, the RP signal of ZC^+-PI-NI^- shows no correlation between its formation and the decay of the triplet precursor, ^{3}*ZCX. The lack of such a correlation indicates that the singlet-initiated route is the active one.

An additional spectral parameter, which is of substantial importance for understanding the spin dynamics is the phase inversion of the time-evolved EPR spectra. Phase inversion usually indicates the participation of two IET routes, e.g., a singlet-initiated RP that can be accompanied by a triplet- initiated RP.[21] The latter spectrum starts to appear at later times. At these low temperatures the TREPR spectrum of ZC^+-PI-NI^- (not shown) does not exhibit a phase inversion with respect to time. This immediately suggests that even for the case of the lowest energy triad (Figure 7), ^{3}*ZCPINI, lies below that of ZC^+-PI-NI^- confirming that the charge separation is not initiated at any time by ^{3}*ZCPINI.

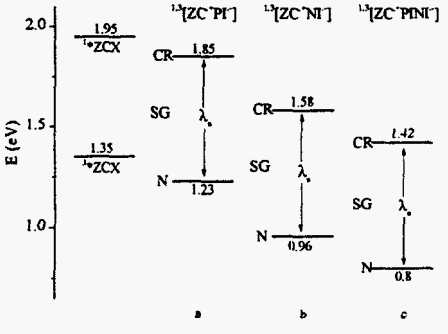

Figure 7. The temperature and phase dependent energy levels of the model systems are shown

Upon increasing the temperature into the soft crystalline phase of E-7, additional features are noticed in the TREPR spectra. The TREPR spectra at 240 K of photoexcited ZCPI and ZCNI are shown in Figure 8. The spectra consist of two components i.e., narrow signals, which are superimposed on broad ones. The broad spectra are attributed to the triplet, ^{3}*ZCX, while the narrow ones are those of the RPs, which are

generated via the routes shown in Figure 3. While in ZCPI only the broad spectrum attributed to the triplet ^{3}*ZCPI is observed, a mixture of triplet and RP spectra are detected for ZCNI. Finally, only RP spectra are detected for ZCPINI (not shown). Additional features for the dyads are the absence of a correlation between the triplet decay and RP formation and the clear phase inversion noticed in the RP spectra. Absorption/emission (a/e) → emission/absorption (e/a) in the case of ZC^+-NI^- (Figure 8) and e/a → a/e in the case of ZC^+-PI-NI^-. As mentioned above the phase inversion corresponds to the existence of two routes for producing the RP states, singlet-initiated followed by triplet-initiated. Therefore, this clearly. indicates that the RP production obeys the energy level diagram shown in Figure 7. The opposite signs of the phase inversion in ZCNI vs ZCPINI are due to the different polarization mechanisms (see below). Nevertheless, both molecules exhibit singlet-initiated spectra followed by triplet-initiated ones. The absence of a triplet spectrum in the case of ZCPINI becomes clear as ^{3}*ZCPINI is depleted rapidly to form the triplet-initiated charge-separated state.

Further increase in temperature to 250 K (just before the appearance of the nematic phase) results in further spectral changes, which are in full agreement with Figure 7. At this temperature, ZCPI shows both triplet and RP spectra, that change phase relatively late in time; ZCNI exhibits less intense triplet spectra accompanied by RP spectra that change phase quite early in time; and finally ZCPINI exhibits intense a/e RP spectra, that do not show any phase inversion. These observations imply that as the triplet-initiated mechanism starts to dominate the spectra, the singlet-initiated spectra are short-lived and in the case of ZCPINI it is below the time resolution of the EPR experiment.

We attribute the appearance of triplet-initiated RPs in the soft glass phase to an increase of the solvent reorganization energy, λ_s, which allows the RP states to be tuned over a wide temperature interval.[25,37-40] The change in the energies of the RPs can be quantified at those temperatures where some of the RPs show evidence for triplet initiation, while the other RPs at higher energies (less driving force) continue to show only the singlet-initiated RPs. This permits bracketing the solvation energies with an error no greater than the difference in the charge separation driving forces, when a triplet-initiated RP pair begins to be observed (Figure 7). For example, the triplet-initiated RPs of both ZC^+-NI^- and ZC^+-PI-NI^- are first observed at 240 K in E-7, which implies that the energy level of ZC^+-NI^- is below ^{3}*ZCX (1.35 eV, Figure 7). Thus, a minimum energy level change for ZC^+-NI^- (and for all the RPs) in the 240 K soft glass relative to the crystalline phase, where E_{RP} = 1.58 eV for ZC^+-NI^-, is -0.23 eV. The energy level change of the three RPs also cannot not be any greater than -0.5 eV, because this would result in triplet-initiated RP formation in ZCPI, which does not occur at 240 K (Figures 7 and 8). At 250 K the triplet-initiated TRP, i.e., ^{3}[ZC^+-PI^-] is observed, now making -0.5 eV the minimum E_{RP} change at this temperature for the RPs. As a result, the reorganization energy of the soft glass at 250 K is already sufficient to produce E_{RP} values similar to those in the isotropic phase of E-7 (Table 1).

Further increase of the temperature, deep into the nematic phase of E-7, results in spectra that are practically the same as those observed in the upper limit of the soft glass region. In terms of the energy-level diagrams (Figure 7), such a temperature change only slightly decreases the RP energies and does not significantly alter the singlet- and triplet- initiated RP production already

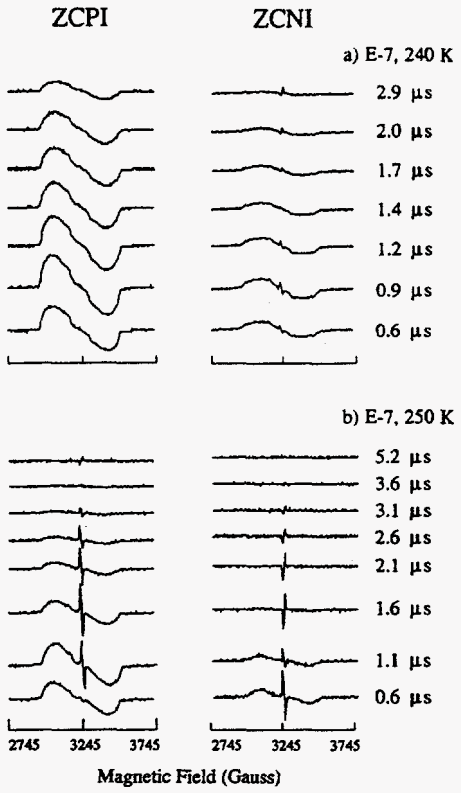

Figure 8. Direct-detection TREPR spectra (triplets and RPs), for different times after the laser pulse, of the photoexcited dyads in the soft glass of E-7 at a)240K and (b) 250K.

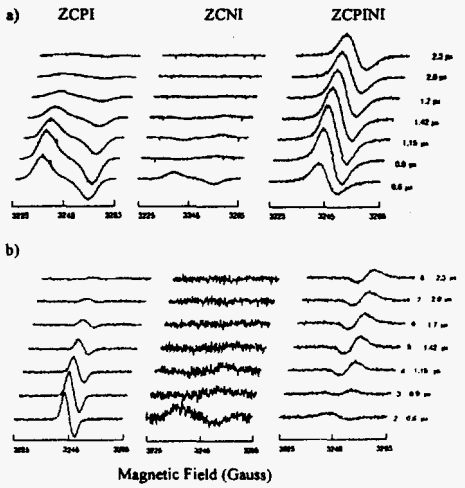

Figure 9. Direct-detection TREPR spectra (RPs), for different times after the laser pulse, of the photoexcited molecules in the nematic phase of: (a) E-7 and (b) ZLI-1167.

observed in the soft glass. Thus, the spectra shown in Figure 9, clearly illustrate the main theme of this work. The TRP spectra of ^{3}[ZC$^+$-PI$^-$] are in a/e mode indicating singlet-initiated spectra, which eventually change into triplet-initiated RPs, i.e., e/a at relatively late times (not shown). On the other hand, the TRP spectrum of ^{3}[ZC$^+$-NI$^-$] starts with an a/e pattern, that changes early in time into an e/a spectrum. In other words, both mechanisms are in operation for both dyads. Finally, the RP spectra of ZC$^+$-PI-NI$^-$ exhibit an a/e pattern, typical of a CRP spectrum that is initiated by the triplet precursor and is consistent with the large driving force from the photoexcited triplet of ZCPINI. The even higher driving force from the photoexcited singlet of ZCPINI results in a singlet-initiated CRP that is too short lived to observe by TREPR. To summarize the E-7 results, TREPR spectroscopy shows that the solvent reorganization energy in the upper limit of the soft glass is tuned to nearly that of the entire nematic (fluid) phase.

The maximum change of the energy levels of the RPs in the nematic phase can be determined independently by the following arguments. At 240 K we showed that the E_{RP} change from the crystalline phase for ZC$^+$-NI$^-$ ranged between –0.23 and –0.5 eV (i.e., E_{RP} equals 1.08 to 1.35 eV). However, in the nematic phase, the rate of charge separation of triplet-initiated ZC$^+$-PI$^-$ is the same as ZC$^+$-NI$^-$ at 240 K, implying that E_{RP} for ZC$^+$-PI$^-$ also ranges between 1.08 and 1.35 eV. Note that because IET in LCs occurs in the adiabatic regime, the small electronic coupling differences between the molecules is of no significance. The average of this range is 1.22 eV, which agrees remarkably well with the 1.23 eV value calculated for ZC$^+$-PI$^-$ in the isotropic phase of E-7. This corresponds to a 0.6eV stabilization of the ion pair in the fluid phase relative to the crystalline phase.

ZLI-1167 does not have a soft glass phase, but these arguments can also be extended to the smectic and nematic phases. The triplet-initiated RP ^{3}[ZC$^+$-NI$^-$] is first observed in the smectic phase at 299 K, again suggesting a minimum value for the change in RP energies from crystalline to smectic to be -0.23 eV, and the maximum value to be -0.5 eV. The triplet-initiated radical pair of ^{3}[ZC$^+$-PI$^-$] is first observed in the nematic phase at 323 K. It is clear that the triplet-initiated RPs are observed at higher temperatures in ZLI-1167 as compared to E-7. This can be explained by the lack of a soft glass phase in ZLI-1167. In this case, the smectic phase functions as the soft glass phase in E-7. Also, as eq. 1 indicates, the ΔG_{CS} for charge separation can be expected to be less for ZLI-1167 than for E-7, due to a smaller value of ε_s for ZLI-1167.

Finally, since ZLI-1167 has a negative diamagnetic susceptibility and E-7 has a positive diamagnetic susceptibility, the molecules are aligned perpendicular to the magnetic field in ZLI-1167 and parallel to the magnetic field in E-7. The different orientations relative the magnetic field can help to determine the nature of the radical pair mechanism, i.e. is the radical pair a triplet radical pair or a correlated radical pair. Since the spectra are inverted in the two orientations only for the triad (Figure 9), the triad spectra are consistent with a correlated radical pair mechanism. The linewidth of the radical pair spectra for the triad is also narrower than that for the dyads, again indicative of a correlated radical pair mechanism for the triad and a triplet radical pair mechanism for the dyads.

4. CONCLUSIONS

We have shown that charge transfer and charge return are mediated by different molecular motions in liquid crystals just above the nematic to isotropic phase transition. In this region microdomains exist that enable one to study anisotropic solvent effects without the optical scattering that is associated with nematic liquid crystals. Charge return of PNI-PI in 5CB is shown to be controlled by solvent motions associated with microdomain reorientation, due to the excellent correlation with the known reorientation times. The charge separation times in 5CB are shown to be non-adiabatic in nature, due to the fast molecular reorientations that mediate the initial reaction.

The TREPR data of the chlorophyll-like donor acceptor systems permit quantitative analysis of the energy levels of the radical pairs in the crystalline, soft glass, and nematic phases of liquid crystals. Destabilization of the radical pairs by 0.6 ± 0.1 eV occurs in the solid phase relative to the calculated energy levels for a radical pair in an isotropic, polar solvent. The soft glass phase of E-7 is remarkable in that nearly the entire energetic destabilization observed in the solid phase is recovered as the temperature is warmed through the last 25 degrees of the soft glass phase. The nematic phase of E-7 shows very similar radical pair energies compared to the highest temperatures of the soft glass phase. We have also demonstrated that supramolecular systems containing single and multiple step charge transfer molecules have different mechanisms for creation of the radical pair. The dyads studied here show a triplet radical pair mechanism, whereas the triad is characterized by a correlated radical pair mechanism.

5. ACKNOWLEDGMENTS

The work at Argonne was supported by the Division of Chemical Sciences, Office of Basic Energy Sciences, U.S. DOE under contract W-31-109-ENG-38. The research in Israel described herein was supported by U.S.-Israel BSF, Israel Council for Research and Development, by the Volkswagen Stiftung, and by the DFG (Sfb program 337).

6. REFERENCES

1. P. G. Schouten; J. M. Warman; M. P. d. Haas; M. A. Fox; H. L. Pan "Charge Migration in Supramolecular Stacks of Peripherally Substituted Porphyrins", *Nature* **353**, pp. 736-7, 1991.
2. B. A. Gregg; M. A. Fox; A. J. Bard "Photovoltaic Effect in Symmetrical Cells of a Liquid Crystal Porphyrin", *J. Phys. Chem.* **94**, pp. 1586-98, 1990.
3. K. Sutter; J. Hulliger; R. Schlesser; P. Gunter "Photorefractive Properties of 4'-Nitrobenzylidene-3-acetamino-4-methoxyaniline", *Opt. Lett.* **18**, pp. 778-80, 1993.
4. G. P. Wiederrecht; B. A. Yoon; M. R. Wasielewski "High Photorefractive Gain in Nematic Liquid Crystals Doped with Electron Donor and Electron Acceptor Molecules", *Science* **270**, pp. 1794-97, 1995.
5. *Photochemistry in Organized and Constrained Media*; V. Ramamurthy, Ed.; VCH: New York, 1991.
6. R. B. Kress; E. N. Duesler; M. C. Etter; I. C. Paul; D. Y. Curtin "Solid-state resolution of binaphthyl: crystal and molecular structures of the chiral (A)1 form and racemic (B)1 form and the study of the rearrangement of single crystals. Requirements for development of hemihedral faces for enantiomer identification.", *J. Am. Chem. Soc.* **102**, pp. 7709-7714, 1980.
7. S. R. Marder; B. Kippelen; A. K.-Y. Jen; N. Peyghammbarian "Design and synthesis of chromophores and polymers for electro-optic nd photorefractive applications", *Nature (London)* **388**, pp. 845-851, 1997.
8. J. Simon; J.-J. Andre *Molecular Semiconductors: Photoelectrical Properties and Solar Cells*; Springer-Verlag: Berlin, 1985.
9. *The Photosynthetic Reaction Center*; J. Deisenhofer; J. R. Norris, Eds.; Academic: New York, 1993.
10. R. G. Weiss; V. Ramamurthy; G. S. Hammond "Photochemistry in organized and confining media: a model", *Acc. Chem. Res.* **26**, pp. 530-36, 1993.
11. F. D. Saeva; G. A. Reynolds; L. Kaszczuk "Liquid-crystalline cation-radical charge-transfer systems", *J. Am. Chem. Soc.* **104**, pp. 3524-25, 1982.
12. G. P. Wiederrecht; W. A. Svec; M. R. Wasielewski "Differential control of intramolecular charge separation and recombination rates using nematic liquid crystal solvents", *J. Am. Chem. Soc.* **119**, pp. 6199-6200, 1997.
13. M. R. Wasielewski; G. L. G. III; M. P. O'Neil; W. A. Svec; M. P. Niemczyk; L. Prodi; D. Gosztola, "Solvent Effects on the Rate vs. Free Energy Dependence of Photoinduced Charge Separation in Fixed-Distance Donor-Acceptor Molecules", *Dynamics and Mechanisms of Photoinduced Electron Transfer and Related Phenomena*; N. Mataga, T. Okada, H. Masuhara, Eds.; Elsevier: New York, 1992.
14. N. S. Sariciftci; U. Lemmer; D. Vacar; A. J. Heeger; R. A. J. Janssen "Polarized Photoluminescence of Oligothiophenes in Nematic Liquid Crystalline Matrices", *Adv. Mater.* **8**, pp. 651-54, 1996.
15. G. P. Wiederrecht; B. A. Yoon; M. R. Wasielewski "Photorefractive Liquid Crystals", *Adv. Mat.* **8**, pp. 535-39, 1996.
16. G. P. Wiederrecht; M. R. Wasielewski "Photorefractivity in Polymer-Stabilized Nematic Liquid Crystals", *J. Am. Chem. Soc.* **120**, pp. 3231-3236, 1998.
17. H. Ono; I. Saito; N. Kawatsuki "Photorefractive Bragg diffraction in high- and low-molar-mass liquid crystal mixtures", *Appl. Phys. Lett.* **72**, pp. 1942-44, 1998.
18. I. C. Khoo; H. Li; Y. Liang "Observation of Orientational Photorefractive Effects in Nematic Liquid Crystals", *Opt. Lett.* **19**, pp. 1723-25, 1994.
19. I. C. Khoo *Liquid Crystals: Physical Properties and Nonlinear Optical Phenomena*; Wiley: New York, 1995.
20. E. V. Rudenko; A. V. Sukhov "Photoinduced Electrical Conductivity and Photorefraction in a Nematic Liquid Crystal", *JETP Lett.* **59**, pp. 142-46, 1994.
21. K. Hasharoni; H. Levanon; S. R. Greenfield; D. J. Gosztola; W. A. Svec; M. R. Wasielewski "Radical Pair and Triplet State Dynamics of a Photosynthetic Reaction-Center Model Embedded in Isotropic Media and Liquid Crystals", *J. Am. Chem. Soc.* **118**, pp. 10228-35, 1996.

22. S. R. Greenfield; W. A. Svec; D. Gosztola; M. R. Wasielewski "Multi-Step Charge Separation Following Direct Excitation of a Charge Transfer State in Rod-Like Molecules Based on Aromatic Imides and Diimides.", *J. Am. Chem. Soc.* **118**, pp. 6767-6777, 1996.
23. A. Osuka; H. Yamada; K. Maruyama; N. Mataga; T. Asahi; M. Ohkouchi; T. Okada; I. Yamazaki; Y. Nishimura "Synthesis and Photoexcited-State Dynamics of Aromatic Group-Bridged Carotenoid-Porphyrin Dyads and Carotenoid-Porphyrin-Pyromellitimide Triads", *J. Am. Chem. Soc.* **115**, pp. 9439-9452, 1993.
24. G. P. Wiederrecht; M. P. Niemczyk; W. A. Svec; M. R. Wasielewski "Ultrafast Photoinduced Electron Transfer in a Chlorophyll-Based Triad: Vibrationally Hot Ion Pair Intermediates and Dynamic Solvent Effects", *J. Am. Chem. Soc.* **118**, pp. 81-88, 1996.
25. H. Levanon; K. Hasharoni "Electron and energy transfer in liquid crystals. Time-resolved electron paramagnetic resonance.", *Prog. Reac. Kinet.* **20**, pp. 309-46, 1995.
26. M. R. Wasielewski "Photoinduced Electron Transfer in Supramolecular Systems for Artificial Photosynthesis", *Chem. Rev.* **92**, pp. 435-461, 1992.
27. P. G. d. Gennes; J. Prost *The Physics of Liquid Crystals*; Clarendon Press: Oxford, U.K., 1993.
28. F. W. Deeg; S. R. Greenfield; J. J. Stankus; V. J. Newell; M. D. Fayer "Nonhydrodynamic Molecular Motions in a Complex Liquid: Temperature Dependent Dynamics in Pentylcyanobiphenyl", *J. Chem. Phys.* **93**, pp. 3503-14, 1990.
29. P. Martinoty; F. Kiry; S. Nagai; S. Candau; F. Debeauvais "Viscosity coefficients in the isotropic phase of a nematic liquid crystal.", *J. Phys.* **27**, pp. 159-62, 1977.
30. R. Marcus "On the theory of electron transfer reactions. VI. Unified treatment for homogeneous and electrode reactions", *J. Chem. Phys.* **43**, pp. 679-701, 1965.
31. B. R. Ratna; R. Shashidhar "Dielectric Studies on Liquid Crystals of Strong Positive Dielectric Anisotropy", *Mol. Cryst. Liq. Cryst.* **42**, pp. 113-125, 1977.
32. J. A. Riddick; W. B. Bunger; T. K. Sakano *Organic Solvents: Physical Properties and Methods of Purification*; 4th ed.; John Wiley and Sons: New York, 1986.
33. G. L. Gaines; M. P. O'Neil; W. A. Svec; M. P. Niemczyk; M. R. Wasielewski "Photoinduced electron transfer in the solid state: rate vs. free energy dependence in fixed-distance porphyrin-acceptor molecules.", *J. Am. Chem. Soc.* **113**, pp. 719-21, 1991.
34. H. Oevering; M. N. Paddon-Row; M. Heppener; A. M. Oliver; E. Cotsaris; J. W. Verhoeven; N. S. Hush "Long-range photoinduced through-bond electron transfer and radiative recombination via rigid nonconjugated bridges: distance and solvent dependence.", *J. Am. Chem. Soc.* **109**, pp. 3258-69, 1987.
35. One electron redox potentials are half-wave potentials determined by cyclic voltammetry at a Pt electrode in butyronitrile containing 0.1M tetra-*n*-butylammonium perchlorate. Potentials are given relative to the saturated calomel electrode.
36. Ion pair distances were estimated from structures calculated using a modified MM2 force field within Hyperchem (Hypercube, Waterloo, Ontario)..
37. H. Heitele; P. Finckh; S. Weeren; F. Pollinger; M. E. Michel-Beyerle "Solvent polarity effects on intramolecular electron transfer. 1. Energetic aspects.", *J. Phys. Chem.* **93**, pp. 5173-9, 1989.
38. H. Heitele "Dynamic solvent effects on electron-transfer reactions.", *Angew. Chem. Int. Ed. Engl.* **32**, pp. 359-77, 1993.
39. K. Hasharoni; H. Levanon "Attenuation of Intramolecular Electron Transfer Rates in Liquid Crystals", *J. Phys. Chem.* **99**, pp. 4875-78, 1995.
40. K. Hasharoni; H. Levanon; J. v. Gersdorff; H. Kurreck; K. Mobius "Photo-induced electron transfer in covalently linked donor-acceptor assemblies in liquid crystals. Time-resolved electron paramagnetic resonance.", *J. Chem. Phys.* **98**, pp. 2916-26, 1993.